Patterns of conductivity in excitable automata with updatable intervals of excitations

Andrew Adamatzky
University of the West of England, Bristol, United Kingdom
(Received 25 July 2012; published 7 November 2012)

We define a cellular automaton where a resting cell excites if number of its excited neighbors belong to some specified interval and boundaries of the interval change depending on ratio of excited and refractory neighbors in the cell's neighborhood. We calculate excitability of a cell as a number of possible neighborhood configurations that excite the resting cell. We call cells with maximal values of excitability conductive. In exhaustive search of functions of excitation interval updates we select functions which lead to formation of connected configurations of conductive cells. The functions discovered are used to design conductive, wirelike, pathways in initially nonconductive arrays of cells. We demonstrate that by positioning seeds of growing conductive pathways it is possible to implement a wide range of routing operations, including reflection of wires, stopping wires, formation of conductive bridges, and generation of new wires in the result of collision. The findings presented may be applied in designing conductive circuits in excitable nonlinear media, reaction-diffusion chemical systems, neural tissue, and assemblies of conductive polymers.

DOI: 10.1103/PhysRevE.86.056105 PACS number(s): 82.40.Ck, 89.75.Kd, 89.70.−a

I. INTRODUCTION

Excitable cellular automata are well-endowed tools for studying complex phenomena of spatiotemporal physical, chemical, and biological systems [1,2], prototyping of chemical media [3,4], reaction-diffusion computers [5], studying calcium wave dynamics [6], and chemical turbulence [7].

In a classical Greenberg-Hasting [8] automaton model of excitation a cell takes three states: reseting, excited, and refractory. A resting cell becomes excited if number of excited neighbors exceeds a certain threshold, an excited cell becomes refractory, and a refractory cell returns to its original resting state. In Ref. [9] we introduced a bit more exotic cellular automaton, where a resting cell is excited if a number of its excited neighbors belongs to some fixed interval $[\theta_1,\theta_2]$. The interval $[\theta_1,\theta_2]$ is called an excitation interval. For a two-dimensional cellular automaton with an eight-cell neighborhood boundaries of the excitation interval are between 1 and 8: $1 \leqslant \theta_1 \leqslant \theta_2 \leqslant 8$. By tuning θ_1 and θ_2 we control automata dynamics and evoke target and spiral waves, stationary excitation patterns, and mobile localizations [5].

How does excitation dynamics change if we allow boundaries of the excitation interval to change during the automaton development? We partially answered the question in Ref. [10] by making the interval $[\theta_1^t(x),\theta_2^t(x)]$ of every cell x dynamically updatable at every step t depending on state of the cell x and numbers of excited and refractory neighbors in the cell x's neighborhood. We found that excitable cellular automata with dynamical excitation intervals exhibit a wide range of space-time dynamics based on an interplay between propagating excitation patterns and excitability of cells modified by the excitation patterns. Such interactions lead to formation of standing domains of excitation, stationary waves, and localized excitations. We analyzed morphological and generative diversities of the functions studied and characterized the functions with highest values of the diversities.

Excitable cellular automata with dynamical intervals of excitation can be considered as discrete phenomenological models, or rather conceptual analogs, of memristive media and excitable chemical medium computers.

A. Memristive medium

The memristor, a passive resistor with memory, is a device whose resistance changes depending on the polarity and magnitude of a voltage applied to the device's terminals and the duration of this voltage's application. Its existence was theoretically postulated by Leon Chua in 1971 based on symmetry in integral variations of Ohm's laws [11–13]. The first experimental prototypes of memristors are reported in Refs. [14–16]. An importance, and the great pragmatic value, of memristors is that one can design logically universal, or functionally complete, circuits composed entirely of the memristors. Potential unique applications of memristors are in spintronic devices, ultradense information storage, neuromorphic circuits [17], and programmable electronics [18], designing binary arithmetical circuits with polymer organic memristors [19].

Despite a phenomenal number of results in memristors produced literally every week there are insufficient findings on phenomenology of spatially extended nonlinear media with hundreds of thousands of locally connected memristive elements. Three cellular automaton models of a memristive medium have been suggested so far:

(1) Itoh-Chua memristor cellular automata, where a cellular automaton lattice is actually designed with memristors [20]

(2) Adamatzky-Chua model of memrisitive cellular automata based on structurally dynamic cellular automata [21]

(3) Semimemristive automata [22].

Itoh-Chua and Adamatzky-Chua models imitate memristive properties of links, connections between cells of automata arrays, but not the cells themselves. The semimemristive automata bring memristivity into cells [22]: Links between cells are always "conductive," but cells themselves can take nonconductive, or refractory, states. The semimemristive automata are excitable cellular automata with retained refractoriness.

In the present paper, an excitability of a cell is calculated as a number of possible neighborhood configurations that excite the resting cell. *Cells with maximal values of excitability are called conductive.* We represent conductivity of a cell x via

boundaries of its excitation interval $[\theta_1(x),\theta_2(x)]$. We excite the cellular automaton, wait till the perturbation spreads and boundaries of excitation intervals of cells are updated, and then select cells with the highest values of excitability. The configurations of conductive cells form conductive pathways by analogy with the formation of conductive pathways in disordered networks of organic memristors [23]. In automata studied polarity of a direct current applied to a cell x is imitated by excited and refractory neighbors of x, and current intensity is represented by a ratio of excited and refractory neighbors.

B. Ensembles of Belousov-Zhabotinsky vesicles

Excitable reaction-diffusion computers, especially those based on a Belousov-Zhabotinsky (BZ) reaction, employ principles of a collision-based computing [5]. Wave fragments collide in a "free" space and change their velocity vectors as the result of the collision. When input and output waves are interpreted as logical variables, the site of the waves' collision can be seen as a logical gates. Wave fragments, similar to dissipative solitons [24], are inherently unstable: They either collapse or explode. A way to overcome the problem of wave fragments' instability was suggested in Refs. [25–27]: a subdivision of the computing substrate into interconnected compartments, so-called BZ vesicles, and allowing waves to collide only inside the compartments. Each BZ vesicle has a membrane that is impassable for excitation. A pore, or a channel, between two vesicles is formed when two vesicles come into direct contact. The pore is small such that when a wave passes through the pore there is insufficient time for the wave to expand or collapse before interacting with other waves entering through adjacent pores, or sites of contact.

It has been observed in chemical laboratory experiments with BZ vesicles [28] that waves of oxidation induced by

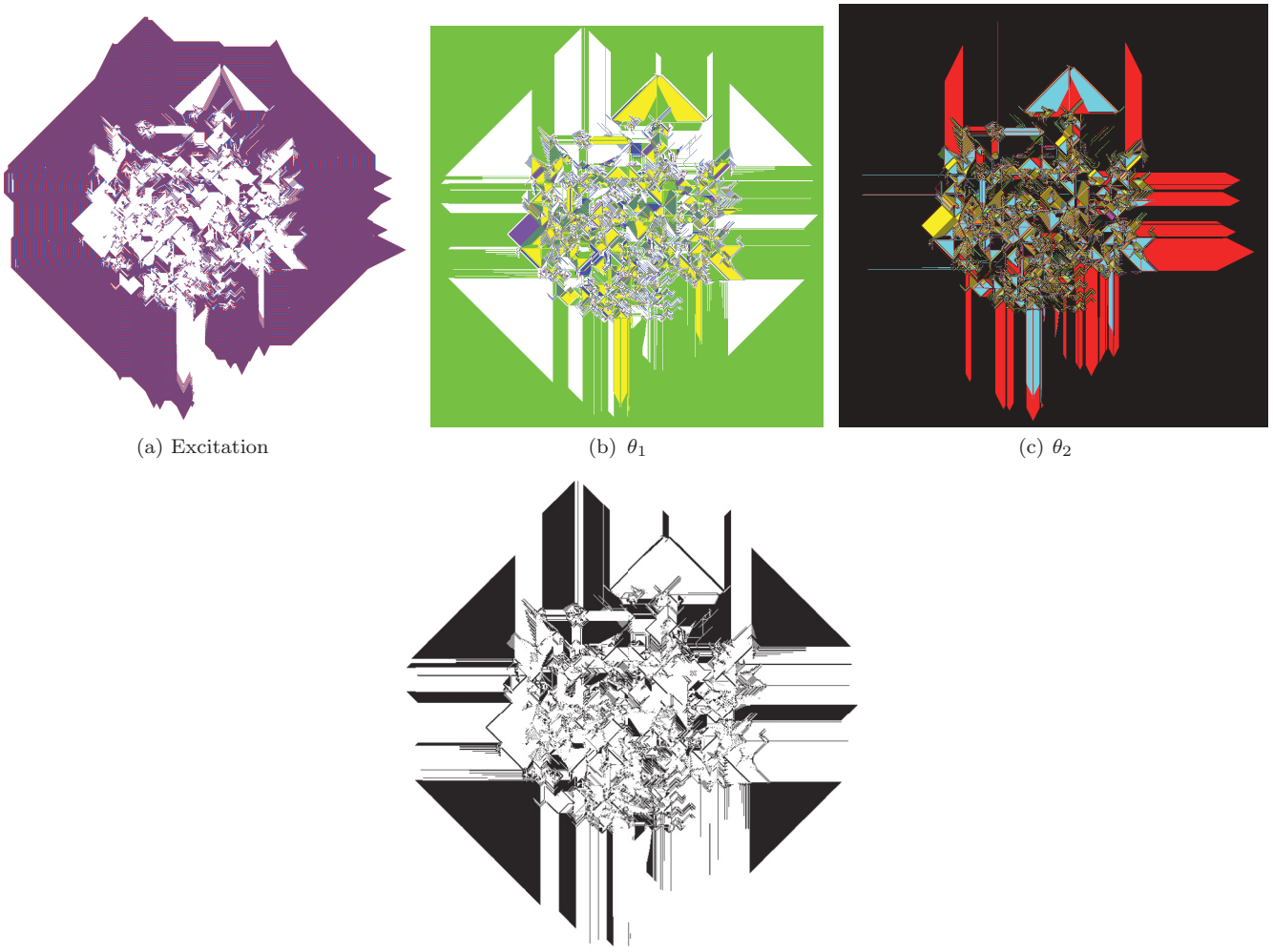

(a) Excitation (b) θ_1 (c) θ_2

(d) Conductivity

FIG. 1. (Color online) Snapshots of (a) excitation pattern, (b) configuration of lower boundary θ_1 of excitation interval, (c) configuration of upper boundary θ_2 of excitation interval, (d) configuration of conductivity of cellular automaton governed by function $E(-1,1,0,-1)$. Array of 880×880 cells evolved for 440 steps. Initially cells inside a disk radius 200 are assigned excited states with probability 10^{-3}. Cell states in (a) are represented by colours and gray levels as follows: excited state $+$ is red (c. 76 gray), resting state is white and refractory state $-$ is blue (c. 28 gray). Color values of excitation interval boundaries θ_1 (b) and θ_2 (c) are following: 1 is white, 2 is green or 150 gray, 3 is yellow or 226 gray, 4 is blue or 28 gray, 5 is magenta or 104 gray, 6 is cyan or 178 gray, 7 is red or 76 gray, and 8 is black. Conductive cells in (d) are black, and nonconductive are white.

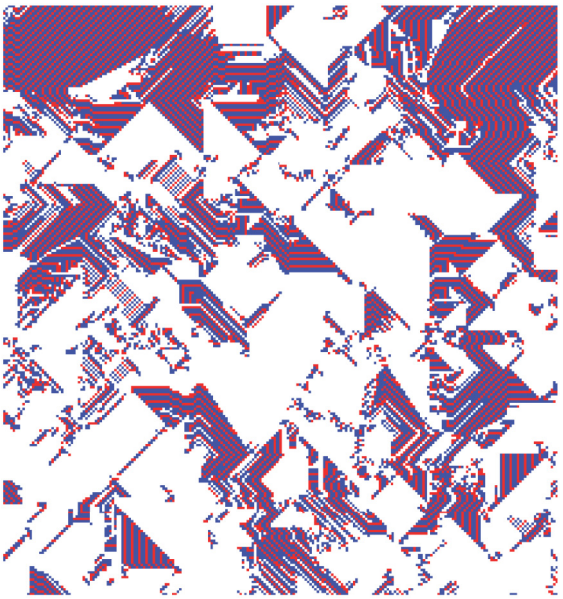

FIG. 2. (Color online) Enlarged part of excitation pattern from Fig. 1(a).

external stimulation, e.g., with a silver wire, propagating in the initially resting BZ medium may cause changes in the excitability of BZ vesicles (not just refractoriness but excitability in the long run). Excitability of BZ vesicles can increase after the first round of the oxidation wave propagation. A cellular automaton model designed in the present paper gives a phenomenological snapshot of an ensemble of regularly arranged BZ vesicles (imitated by cells), which change their long-term excitability after being subjected to propagating waves of excitation.

The paper is structured as follows. We define an excitable cellular automata with dynamically updated boundaries of excitation intervals in Sec. II. Configurations of conductivity generated by the automata are analyzed in Sec. III. The functions which produce fully conductive configurations are selected in an exhaustive search. Section IV demonstrates how to design conductive wirelike pathways by positions' seeds of excitation. Potential further developments are outlined in Sec. V.

II. EXCITATION-CONTROLLED EXCITATION INTERVALS

Let L be a two-dimensional orthogonal array of finite state machines, or cells, x^t and x^{t+1} states of a cell x at time steps t and $t+1$, and $\sigma_+^t(x)$ a sum of excited neighbors in cell x's

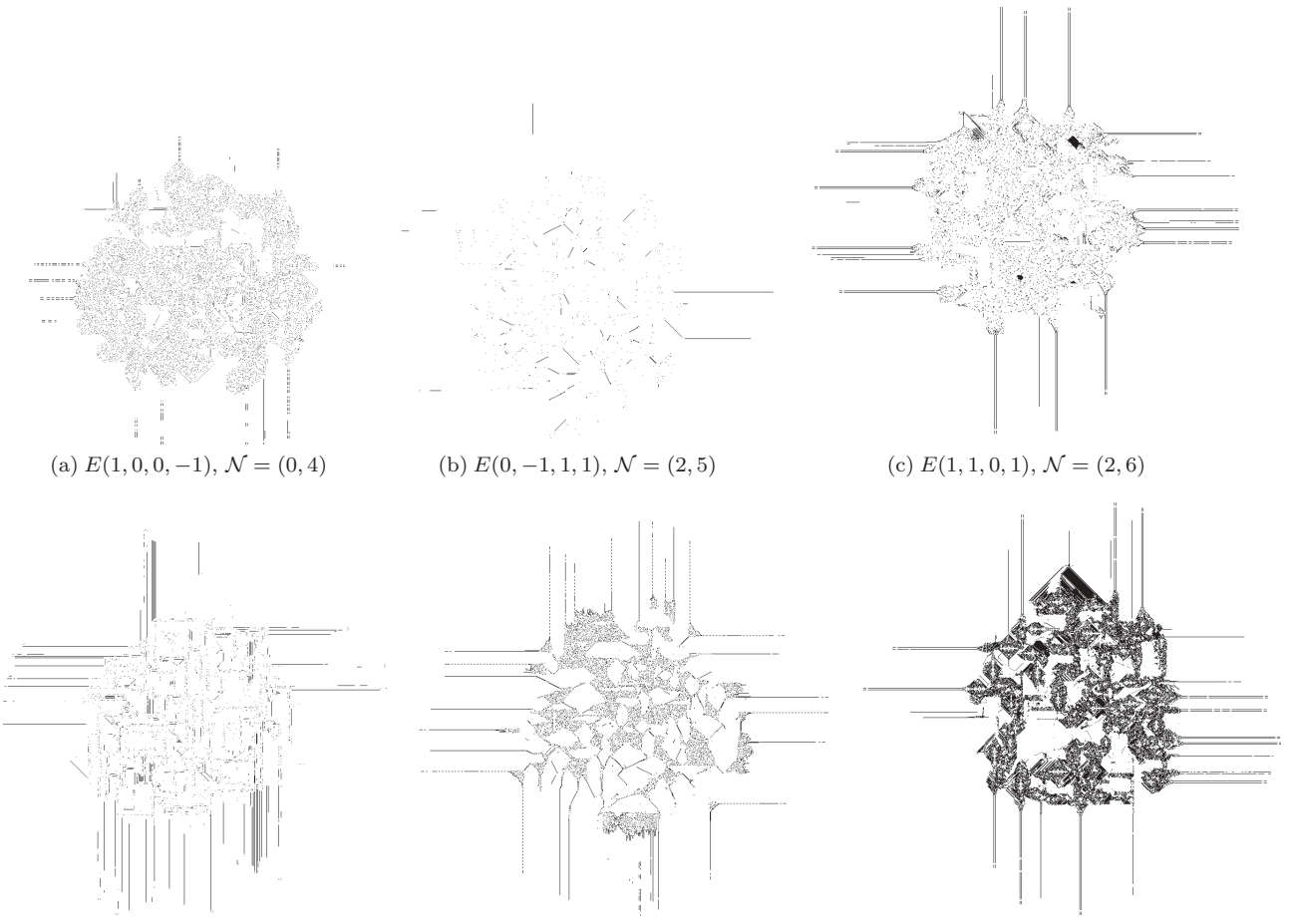

(a) $E(1,0,0,-1)$, $\mathcal{N}=(0,4)$ (b) $E(0,-1,1,1)$, $\mathcal{N}=(2,5)$ (c) $E(1,1,0,1)$, $\mathcal{N}=(2,6)$

(d) $E(1,1,1,1)$, $\mathcal{N}=(2,7)$ (e) $E(0,-1,1,-1)$, $\mathcal{N}=(2,8)$ (f) $E(1,-1,0,1)$, $\mathcal{N}=(5,0)$

FIG. 3. Examples of conductivity configurations.

eight-cell neighborhood, $u(x) = \{y : |x - y|_{L_\infty} = 1\}$. Cell x updates its state by the rule $x^{t+1} = f(u(x))$, where cell-state update function f is represented as

$$x^{t+1} = \begin{cases} +, & \text{if } x^t = \circ \quad \text{and} \quad \sigma_+^t(x) + \in \left[\theta_1^t(x), \theta_2^t(x)\right] \\ -, & \text{if } x^t = + \\ \circ, & \text{otherwise} \end{cases}. \tag{1}$$

A resting cell is excited if a number of its neighbors belongs to excitation interval $[\theta_1^t(x), \theta_2^t(x)]$, where $1 \leqslant \theta_1^t(x), \theta_2^t(x) \leqslant 8$. The boundaries $\theta_1^t(x)$ and $\theta_2^t(x)$ are dynamically updated depending on cell x's state and numbers of x's excited $\sigma_+^t(x)$ and refractory $\sigma_-^t(x)$ neighbors. A natural way to update boundaries is by increasing or decreasing their values as follows:

$$\begin{aligned} \theta_1^{t+1}(x) &= \xi\left\{\theta_1^t(x) + \Delta_1 \phi[\sigma_+^t(x) - \sigma_-^t(x)]\right\}, \\ \theta_2^{t+1}(x) &= \xi\left\{\theta_2^t(x) + \Delta_2 \phi[\sigma_+^t(x) - \sigma_-^t(x)]\right\}, \end{aligned} \tag{2}$$

where

$$\Delta_1 = \begin{cases} T_1, & \text{if } x = + \\ T_3, & \text{if } x = - \\ 0, & \text{if } x = 0 \end{cases} \qquad \Delta_2 = \begin{cases} T_2, & \text{if } x = + \\ T_4, & \text{if } x = - \\ 0, & \text{if } x = 0 \end{cases} \tag{3}$$

and $\phi(a - b) = 1$ if $a > b$, 0 if $a = b$ and -1 if $a < b$, and $\xi(a) = 1$ if $a < 1$ and 8 if $a > 8$. Boundaries of excitation interval $[\theta_1^t(x), \theta_2^t(x)]$ are updated independently of each other. Rules of excitation intervals update are determined by values of $T_1, \ldots, T_4$. We therefore address the functions as tuples $E(T_1, T_2, T_3, T_4)$, which range from $E(-1,-1,-1,-1)$ to $E(1,1,1,1)$.

Excitability $\mathcal{E}(\theta_1(x), \theta_2(x))$ of a cell x with excitation interval $[\theta_1(x), \theta_2(x)]$ is measured as a number of all possible local configurations, which have a sum of excited cells lying in the excitation interval $[\theta_1(x), \theta_2(x)]$:

$$\mathcal{E}(\theta_1, \theta_2) = |\{w \in \{\circ, +, -\}^8\} : f(w) = +|. \tag{4}$$

Two highest excitability values are reached by cells with excitation intervals [1,7] and [1,8], $\mathcal{E}(1,7) = 6304$ and $\mathcal{E}(1,8) = 6305$. We assume a cell x is conductive if $\mathcal{E}(\theta_1(x), \theta_2(x)) > 6300$. Connectivity of the configurations of cells with maximal excitability is considered to be an analog of conductivity of the whole cellular array. The connectivity is estimated using a standard bucket fill algorithm.

Definition 1. We call conductivity configuration diameter D fully conductive if there is a path between two sites lying at distance D from each other, and over 90% of sites are reached from any given site.

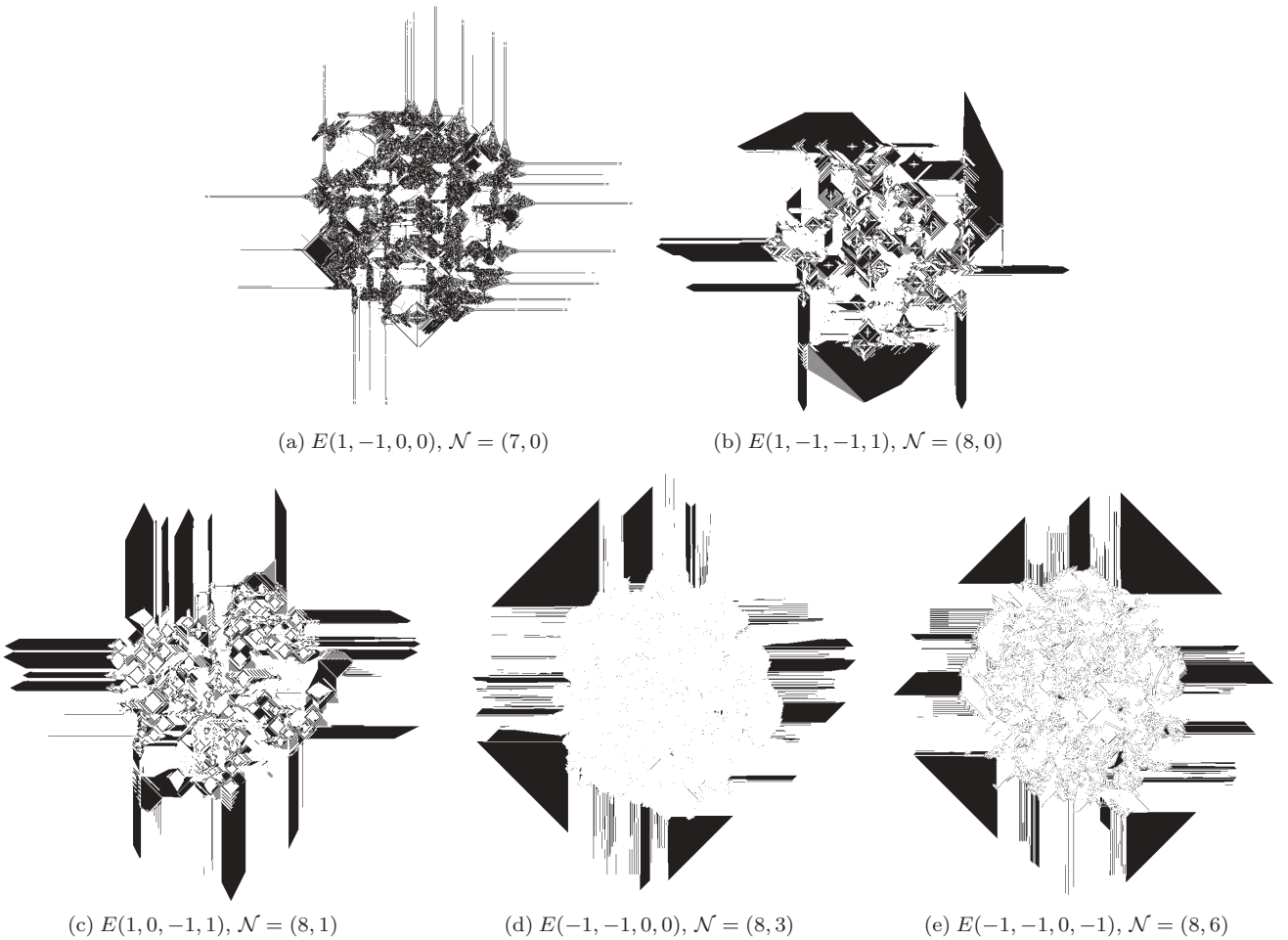

(a) $E(1,-1,0,0)$, $\mathcal{N} = (7,0)$ (b) $E(1,-1,-1,1)$, $\mathcal{N} = (8,0)$

(c) $E(1,0,-1,1)$, $\mathcal{N} = (8,1)$ (d) $E(-1,-1,0,0)$, $\mathcal{N} = (8,3)$ (e) $E(-1,-1,0,-1)$, $\mathcal{N} = (8,6)$

FIG. 4. Examples of conductivity configurations.

We study formation of conductive pathways in an initially nonconductive medium. Therefore, in experiments we considered initial conditions $\theta_1^0(x) = 2$ and $\theta_2^0(x) = 8$ for any x. The excitation interval [2,8] gives a cell excitability 5281, which is below a threshold adopted as an indicator of conductivity.

We excite a disk radius 200 cells with a random configuration of excited states. Let p be a probability for a cell x to be assigned an excited state at $t = 0$ and one of its neighbors, chosen at random, also assigned an excited state. Two neighboring excited cells are a minimal size of perturbation due to $\theta_1^0(x) = 2$. We considered $p = 10^{-3}$ and $p = 0.1$. Initially cells inside a disk radius 200 are assigned excited states with probability p.

In each trial we allowed the cellular automaton to develop for 440 iterations and then analyzed configurations of conductivity. Size of cellular arrays was chosen large enough for a perturbation front to never reach the array's boundaries in 440 steps, so there are no influences of boundary conditions.

III. CONDUCTIVE CONFIGURATIONS

Sites of initial random excitations generate waves, localizations, and other traveling patterns of excitation. The patterns either stay localized or merge and propagate outwards in the initially perturbed region. The patterns of excitation update boundaries of excitation intervals of cells they excited. An example of cellular automaton, function $E(-1,1,0,-1)$, and its development is shown in Fig. 1. Waves of excitation propagate from the perturbation sites [Figs. 1(a) and 2], leaving somewhat fiber-like trails and extended domains of lower θ_1 [Fig. 1(b)] and upper θ_2 [Fig. 1(c)] boundaries of excitation intervals. These are reflected in solid domains of conductivity partially linked with wirelike conductive paths [Fig. 1(d)]. Excitation waves originating from different sites of perturbation merge outside the stimulation disk and propagate further as almost connected packet of target waves [Fig. 1(a)]. These waves leave triangular solid domains of conductivity behind [Fig. 1(d)].

A. Classes of connectivity

We characterize local connectivity of conductivity configurations using $\nu_{\max}$, a number of conductive neighbors of a conductive cell that occurred most frequently in the configuration of conductivity, and $\nu_{\min}$, which occurred less frequently. For initial probability of excitation 10^{-3} we have 12 classes of local connectivity, and the functions are grouped by values $\mathcal{N} = (\nu_{\max}, \nu_{\min})$ of their conductivity configurations. Examples of configurations of conductivity generated by functions from these classes are shown in Figs. 3 and 4:

(1) $\mathcal{N} = (0,0)$: $E(0,-1,0,-1)$, $E(0,-1,0,0)$, $E(0,-1,0,1)$, $E(0,0,0,-1)$, $E(0,0,0,0)$, $E(0,0,0,1)$, $E(0,1,0,-1)$, $E(0,1,0,0)$, $E(0,1,0,1)$

(2) $\mathcal{N} = (0,4)$: $E(1,0,0,-1)$, $E(1,1,0,-1)$ [Fig. 3(a)]

(3) $\mathcal{N} = (2,5)$: $E(0,-1,1,1)$ and $E(1,1,0,0)$ [Fig. (3 b)]

(4) $\mathcal{N} = (2,6)$: $E(1,1,0,1)$ [Fig. 3(c)]

(5) $\mathcal{N} = (2,7)$: $E(0,0,1,1)$, $E(0,1,1,1)$, $E(1,-1,0,-1)$, $E(1,-1,1,-1)$, $E(1,-1,1,0)$, $E(1,-1,1,1)$, $E(1,0,1,-1)$, $E(1,0,1,0)$, $E(1,0,1,1)$, $E(1,1,1,-1)$, $E(1,1,1,0)$, $E(1,1,1,1)$ [Fig. 3(d)]

(6) $\mathcal{N} = (2,8)$: $E(0,-1,1,-1)$, $E(0,-1,1,0)$, $E(0,0,1,-1)$, $E(0,0,1,0)$, $E(0,1,1,-1)$, $E(0,1,1,0)$ [Fig. 3(e)]

(7) $\mathcal{N} = (5,0)$: $E(1,-1,0,1)$, $E(1,0,0,1)$ [Fig. 3(f)]

(8) $\mathcal{N} = (7,0)$: $E(1,-1,0,0)$, $E(1,0,0,0)$ [Fig. 4(a)]

(9) $\mathcal{N} = (8,0)$: $E(-1,-1,-1,-1)$, $E(-1,-1,1,1)$, $E(-1,0,-1,-1)$, $E(-1,0,0,-1)$, $E(-1,0,0,0)$, $E(-1,1,0,-1)$, $E(-1,1,0,0)$, $E(-1,1,0,1)$, $E(0,-1,-1,-1)$, $E(0,-1,-1,0)$, $E(0,-1,-1,1)$, $E(0,0,-1,0)$, $E(0,0,-1,1)$, $E(0,1,-1,1)$, $E(1,-1,-1,-1)$, $E(1,-1,-1,0)$, $E(1,-1,-1,1)$, $E(1,0,-1,0)$, $E(1,1,-1,1)$ [Fig. 4(b)]

(10) $\mathcal{N} = (8,1)$: $E(-1,-1,-1,0)$, $E(-1,-1,-1,1)$, $E(-1,0,-1,0)$, $E(-1,0,-1,1)$, $E(-1,1,-1,0)$, $E(-1,1,-1,1)$, $E(1,0,-1,1)$ [Fig. 4(c)]

(11) $\mathcal{N} = (8,3)$: $E(-1,-1,0,0)$, $E(-1,-1,0,1)$, $E(-1,-1,1,0)$, $E(-1,0,1,1)$, $E(-1,1,-1,-1)$, $E(-1,1,1,1)$, $E(0,0,-1,-1)$, $E(0,1,-1,-1)$, $E(0,1,-1,0)$, $E(1,0,-1,-1)$, $E(1,1,-1,-1)$, $E(1,1,-1,0)$ [Fig. 4(d)]

(12) $\mathcal{N} = (8,6)$: $E(-1,-1,0,-1)$, $E(-1,-1,1,-1)$, $E(-1,0,0,1)$, $E(-1,0,1,-1)$, $E(-1,0,1,0)$, $E(-1,1,1,-1)$, $E(-1,1,1,0)$ [Fig. 4(e)].

Class $\mathcal{N} = (8,0)$ is the largest class, and it has 19 functions. Configurations of conductivity generated by the functions from $\mathcal{N} = (8,0)$ [Fig. 4(b)] are characterized by large solid conductive domains formed either by initial source of excitation, see, e.g., rectangular embedded shapes in Fig. 4(b), or by merging fronts of excitation (solid polygonal domains at the periphery).

The next largest classes are $\mathcal{N} = (2,7)$ and $\mathcal{N} = (8,3)$ [Fig. 4(d)]. Each of them includes 12 functions. Conductivity configurations generated by functions of class $\mathcal{N} = (2,7)$

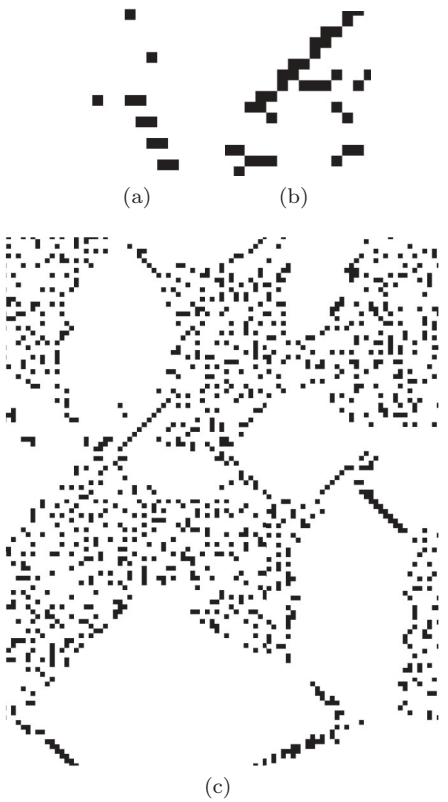

FIG. 5. Fragments of configurations generated by (a) function $E(0,-1,1,1)$ from $\mathcal{N} = (2,5)$, (b) function $E(1,1,0,1)$ from $\mathcal{N} = (2,6)$, (c) function $E(0,1,1,0)$ from $\mathcal{N} = (2,8)$.

consist mainly of isolated line segments of cells in conductive states and pairs or singletons. Configurations generated by functions of $\mathcal{N} = (8,3)$ are made up of solid domains of conductive states and sparsely scattered singletons [Fig. 3(d)].

Classes $\mathcal{N} = (2,5)$ [Fig. 3(b)], $\mathcal{N} = (2,6)$ [Fig. 3(c)], and $\mathcal{N} = (2,7)$ [Fig. 3(d)] pose particular interest because the majority of conductive cells have two conductive neighbors each, and therefore chances of conductive "wires" to be formed could be high.

Configurations generated by functions from $\mathcal{N} = (2,5)$ [Fig. 3(b)] predominantly consist of singletons and pairs of cells in conductive states; the pairs are aligned in staircase-like fashion, but there is no immediate connection between the pairs [Fig. 5(a)]. There are zigzag-like "wires" of conductive states [Fig. 5(b)] in configurations [Fig. 3(c)] generated by the only function $E(1,1,0,1)$ in class $\mathcal{N} = (2,6)$. However, they are present as isolated fragments. Configurations [Fig. 3(e)] generated by function $E(0,1,1,0)$ of class $\mathcal{N} = (2,8)$ consist of clusters of singletons, single conductive cells surrounded by nonconductive neighbors, and pairs of cells in conductive states. The clusters are connected to each other with diagonals of singletons [Fig. 5(c)]. Neither of the functions with $\nu_{\max} = 2$ generate fully conductive configurations but few functions from classes $\mathcal{N} = (7,0)$ and $\mathcal{N} = (8,0)$ do. We study these functions below.

B. Functions generating conductive configurations

Most functions generate only partially conductive configurations of conductivity. Examples of connected clusters are shown in Fig. 6.

Finding 1. For low probability of initial excitation, $p = 10^{-3}$, functions $E(1,0,0,0)$ and $E(1,-1,0,0)$ generate fully conductive configurations. For high probability of initial

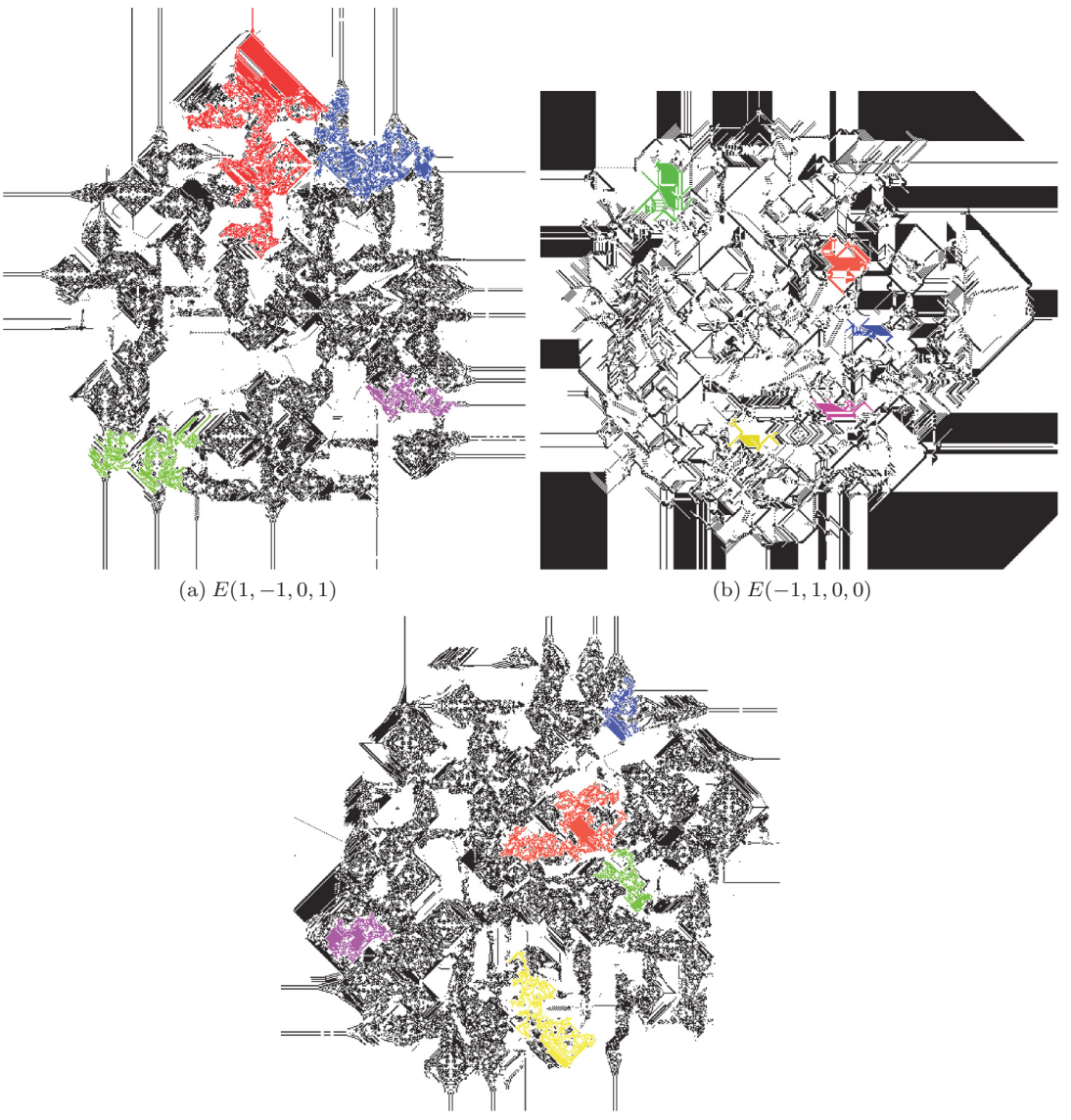

(a) $E(1,-1,0,1)$ (b) $E(-1,1,0,0)$

(c) $E(1,0,0,1)$

FIG. 6. (Color online) Examples of configurations with partially connectivity clusters colored. The clusters are bucket flooded with red, blue, green, magenta, and yellow colors (seen as shades of gray in black and white reproduction).

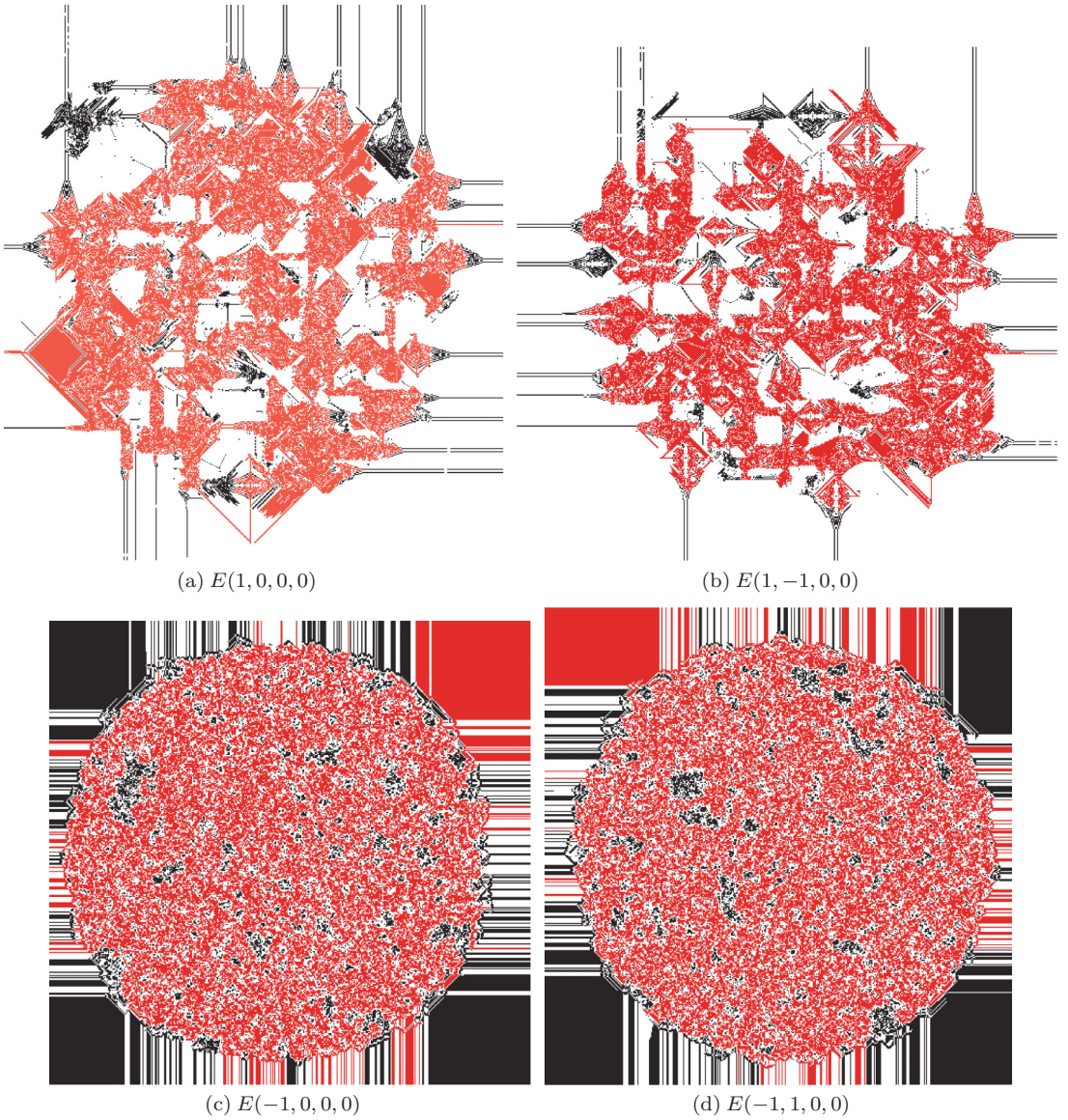

FIG. 7. (Color online) Examples of conductivity configurations generated by functions (a) $E(1,0,0,0)$, (b) $E(1,-1,0,0)$, (c) $E(-1,0,0,0)$, and (d) $E(-1,1,0,0)$. Nonconductive cells are white. Instances of connected clusters of conductive cells are bucket flooded with red (c. 76 gray).

excitations, $p = 0.1$, fully conductive configurations are generated by functions $E(-1,0,0,0)$ and $E(-1,1,0,0)$.

For low probability $p = 10^{-3}$ of initial excitation-only functions $E(1,-1,0,0)$ [Figs. 7(a)] and $E(1,0,0,0)$ generate fully conductive configurations. For initial configurations with high probability of excited cells ($p = 0.1$) only two functions generate conductive configurations: $E(-1,0,0,0)$ [Fig. 7(c)] and $E(-1,1,0,0)$ [Fig. 7(d)]. In all four functions selected values T_3 and T_4 are nil. The values correspond to update of excitation intervals of refractory cells. This is in line with the commonly accepted assumption that in an excitable medium elements in a refractory state are insensitive to states of their neighbors. Mechanics of excitation interval updates of excited cells is illustrated in Fig. 8.

Function $E(1,0,0,0)$ increases lower boundary $\theta_1(x)$ of excitability interval of a cell x when a number of excited neighbors of the cell exceeds a number of refractory neighbors. If a cell has fewer excited neighbors than refractory ones, then the lower boundary of the excitability interval decreases. Function $E(1,-1,0,0)$ increases lower boundary θ_1 and decreases upper boundary θ_2 of the excitability interval of a cell when excited neighbors of the cells are in the majority. If refractory cells dominate in a cell's neighborhood, then θ_1 decreases and θ_2 increases (Fig. 8). Both functions decrease the excitability of a cell when the cell's neighborhood is "overexcited" (prevalence of excited neighbors) and increase the cell's excitability when the cell's neighborhood is "overrefractory" (prevalence of refractory neighbors). Thus they stabilize the excitation dynamics.

Function $E(-1,0,0,0)$ decreases θ_1 when a cell has majority of excited neighbors and increases θ_1 if refractory neighbors dominate. Function $E(-1,1,0,0)$ expands excitation interval

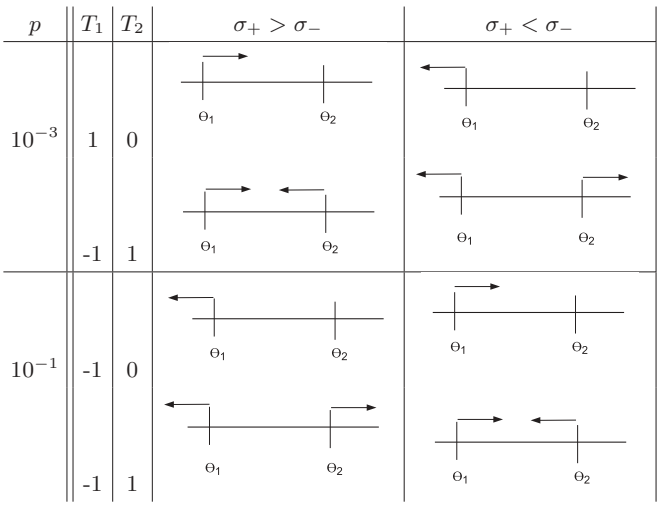

FIG. 8. Mechanics of excitation interval update in functions $E(1,0,0,0)$, $E(1,-1,0,0)$, $E(-1,0,0,0)$ and $E(-1,1,0,0)$. σ_+ is a number of excited neighbors in a cell's neighborhood and σ_- is a number of refractory neighbors.

(θ_1 decreases and θ_2 increases) when there are more excited than refractory neighbors and contracts the excitation interval (θ_1 increases and θ_2 decreases) when refractory neighbors prevail (Fig. 8). The functions increase excitability of cells with "overexcited" neighborhoods and decrease excitability of cells with "overrefractory" neighborhoods. Thus they destabilize the excitation dynamics.

Finding 2. For low probabilities of initial perturbations functions stabilizing excitation dynamics generate conductive configurations, while for high probabilities of initial perturbations functions destabilizing excitation dynamics generate conductive configurations.

Let $E(e_1,e_2,e_3,e_4)$ be a function generating conductive configurations for low probability of excitation in initial configurations and $E'(e'_1,e'_2,e'_3,e'_4)$ the function generating conductive configurations for high probability of excitation in initial configuration. Then

$$E(e_1,e_2,e_3,e_4) = E'(-1\times e'_1,-1\times e'_2,-1\times e'_3,-1\times e'_4).$$

IV. GROWING CONDUCTIVE PATHWAYS WITH FUNCTIONS $E(1-100)$ and $E(1000)$

Let us consider how to route conductive pathways using minimal resources. The pathways can be initiated by exciting the medium. A minimal seed is a pair of cells in excited state ++ or $\begin{smallmatrix}+\\+\end{smallmatrix}$. The seed generates a growing pattern of excitation (Fig. 9). The excitation pattern starts as a target wave [Figs. 9(c)–9(f)]. At a sixth step of development excitation ruptures inside the wave front on its easternmost and westernmost sites [Fig. 9(g)], and propagates along the wave-front boundary inside the target wave [Figs. 9(h)–9(j)]. At a tenth step of the seed's development the excitation reaches the original seed's position [Fig. 9(k)]. Thus the propagating pattern becomes "filled" with persistent excitation activity.

The associated development of configurations of cells in a conductive state is shown in Fig. 10. The seed initiates two types of growing pathways: single chains and double chains of conductive states. For example, a configuration evoked by seed ++ [Fig. 9(a)] exhibits two single chains, growing west and east, and two double chains, growing north and south (Fig. 10). The chains growing north and south increase their lengths by one cell each, speed 1. The chains growing west and east increase by one cell every other step of development, speed 1/2.

The mechanics of formation of conductive pathways is illustrated in Fig. 11. Excited cells having configurations $\begin{smallmatrix}\circ&\circ&-\\\circ&+&\circ\\\circ&-&\circ\end{smallmatrix}$ and $\begin{smallmatrix}-&\circ&\circ\\\circ&+&\circ\\\circ&-&\circ\end{smallmatrix}$ (north and south proximities of the excitation pattern), and configurations $\begin{smallmatrix}\circ&\circ&-\\\circ&+&\circ\\\circ&\circ&-\end{smallmatrix}$ and $\begin{smallmatrix}-&\circ&\circ\\\circ&+&\circ\\-&\circ&\circ\end{smallmatrix}$ (west and east proximities of the excitation patterns) decrease their values of $\theta_1(x)$ from 2 to 1, thus increasing the cells' excitability.

Finding 3. By positioning an additional cell in excited or refractory state nearby the original seed of two excited cells it is possible to generate a wide range of single-thread wires growing into predetermined directions.

Let us consider several examples.

If we excite a cell above the east site of the seed $\begin{smallmatrix}\circ&\circ\\+&+\end{smallmatrix}$, the modified seed $\begin{smallmatrix}\ddagger&\circ\\+&\end{smallmatrix}$ will develop into a growing excitation pattern which generates two chains of cells in conductive states. One chain grows east and another chain grows south. Space-time configurations of excited and refractory cells and conductive cells are shown in Fig. 12. A seed of three excited cells [Fig. 12(a)] develops into an excitation wave fragment propagating southeast [Figs. 12(e), 12(g), and 12(i)]. The wave fragment expands east and south [Figs. 12(k), 12(m), and 12(o)] and resembles an oxidation wave fragment in subexcitable BZ medium [5]. Conductive wires are produced at the sites of excited cells, which have neighborhood configurations $\begin{smallmatrix}\circ&\circ&\circ\\-&+&-\\\circ&\circ&\circ\end{smallmatrix}$ (north corner of the expanding wave fragment) and $\begin{smallmatrix}\circ&-&\circ\\-&+&\circ\\\circ&\circ&\circ\end{smallmatrix}$ (south corner) [Figs. 12(k), 12(m), and 12(o)].

To produce three wires growing north, south and east we excite a neighboring cell northwest of the seed ++ (Fig. 13). The configuration $\begin{smallmatrix}\circ&+&+\\+&+&\circ\\\circ&\circ&\circ\end{smallmatrix}$ of initial excitation generates a wave fragment of excited and refractory states which travels west and expands north and south [Fig. 13(i), 13(k), 13(m), and 13(o)]. A wire growing west is produced by decreasing θ_1 of excited cell with neighborhood $\begin{smallmatrix}+&\circ&-\\-&+&\circ\\+&\circ&-\end{smallmatrix}$ because it has more refractory neighbors (three cells) than excited neighbors (two cells). Wires growing north and south are produced by excited cells having neighborhood configurations $\begin{smallmatrix}\circ&\circ&-\\\circ&+&\circ\\\circ&-&\circ\end{smallmatrix}$ and $\begin{smallmatrix}\circ&-&\circ\\\circ&+&\circ\\\circ&\circ&-\end{smallmatrix}$.

By making the north neighbor of an eastern excited cell of the seed ++ refractory we produce a single chain of conductive cells growing south (Fig. 14). The pattern $\begin{smallmatrix}-&\circ\\+&+\end{smallmatrix}$ [Fig. 14(a)] is transformed into a particle of three excited and three refractory states: $\begin{smallmatrix}\circ&\circ&-\\-&+&\circ\\+&+&\circ\end{smallmatrix}$ [Figs. 14(a), 14(i), 14(k), 14(m), 14(o), 14(q), and 14(s)]. The particle travels south. Its tail leaves a trace of conductive cells [Figs. 14(a) and 14(i)–14(t)] due to excited cell having two refractory neighbors, $\begin{smallmatrix}\circ&-&\circ\\-&+&\circ\\\circ&\circ&\circ\end{smallmatrix}$, and therefore decreasing its θ_1 to 1.

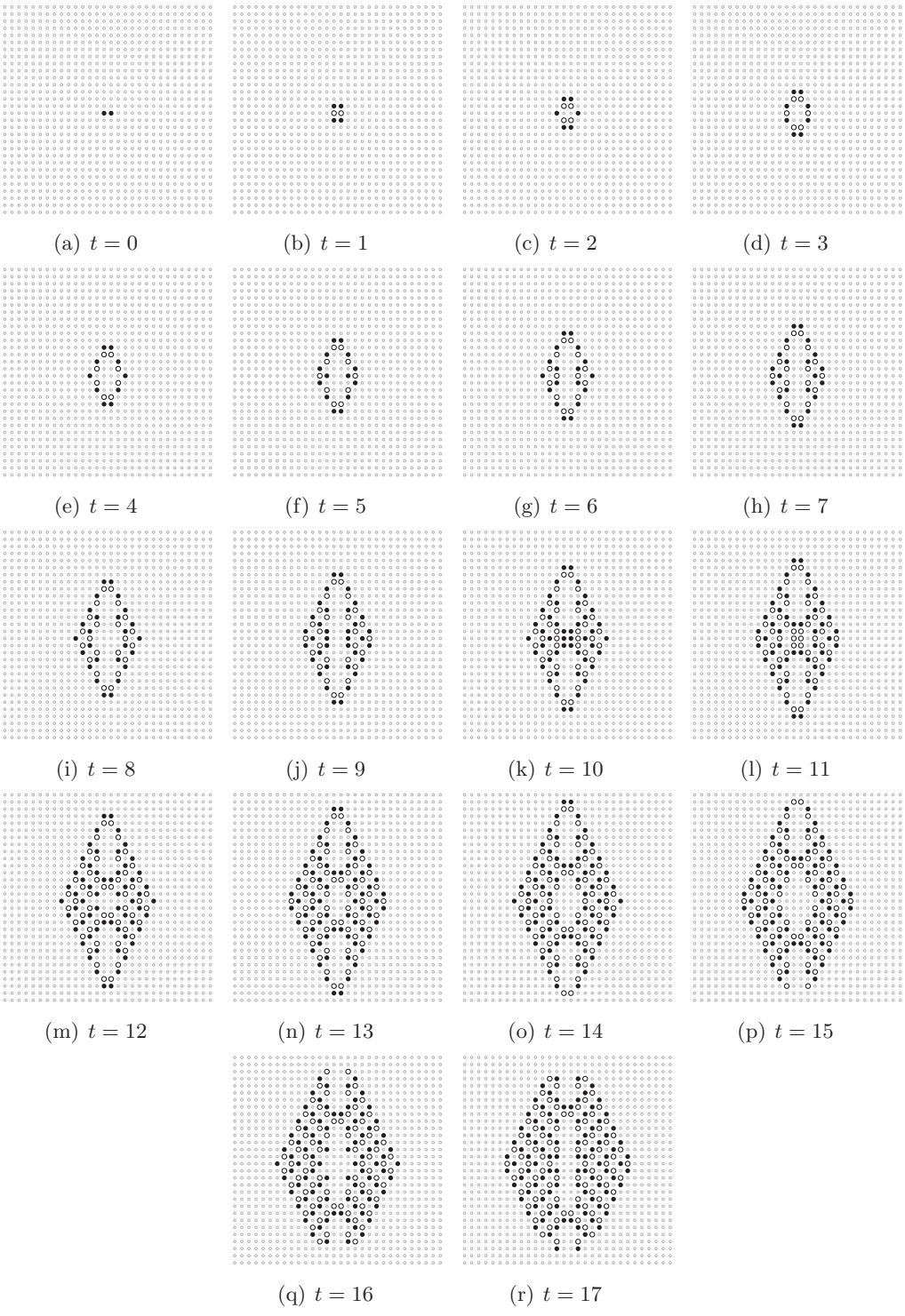

FIG. 9. Snapshots of a growing pattern of excitation developed from a seed of two neighboring cells in excited state. Excited cells are shown by black disks, refractory cells by circles, and resting cells by gray dots.

We have undertaken an exhaustive search of head-on collisions between wires growing north and south (Fig. 15). A wire growing south was generated by seed $\begin{smallmatrix} - \\ + \end{smallmatrix}\begin{smallmatrix} \circ \\ + \end{smallmatrix}$ and a wire growing north by seed $\begin{smallmatrix} + \\ \circ \end{smallmatrix}\begin{smallmatrix} + \\ + \end{smallmatrix}$. At the beginning of each run seeds were placed at distance $C = (h,v)$ from each other, where h is a number of cells along rows and v along columns of cellular array [Fig. 15(a)]. Types of collision outcomes discovered are also illustrated by schemes [Figs. 16(k)–16(r)]. The following basic types are found.

For distance $C = (80,0)$ the wires collide, reflect, and then retract back to their origin sites. After retraction the continuing growing directions opposite to their original velocity vectors. Wire originally growing north grows south, and wire growing south grows north [Fig. 15(b)]. In the same time an additional

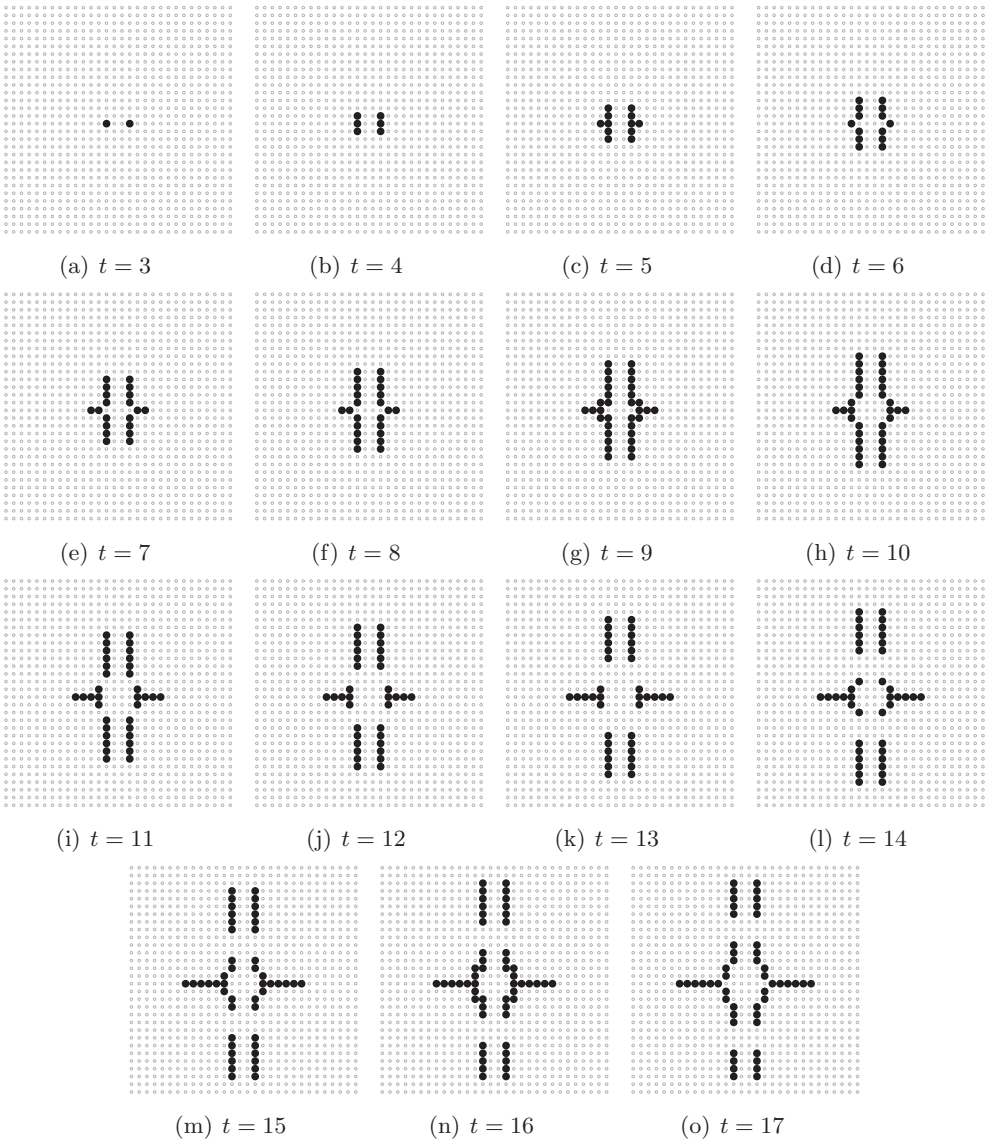

FIG. 10. Snapshot of configuration of conductive cells developed from seed ++.

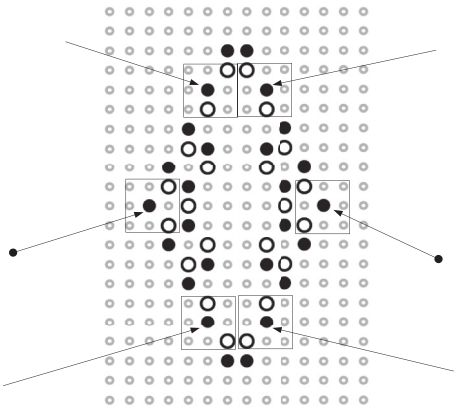

FIG. 11. Configuration of excited (•) and refractory cells (○) with highlighted cells responsible for formation of conductive pathways. Cells where double wire is formed are marked with arrows and a single wire with arrows with disk tops. This configuration develops at the seventh step of the seed's evolution [Fig. 9(h)].

growth seed is formed at the site of the collision between wires, it gives rise to two more wires growing north and south [Figs. 15(b) and 16(k)].

In the situation of a one-cell horizontal shift between seeds' positions, distance $C = (80,1)$, both wires reflect but only the north growing wire (reflected south) continues growing beyond the position of its original seed [Figs. 15(c) and 16(l)]. If there is a two-cell horizontal space between the seeds [Fig. 15(d)], then both wires reflect and continue their growth into reflected directions [Figs. 15(d) and 16(m)].

For distance $C = (80,3)$ both wires reflect as in previous situations; however, only one wire continues growing north (after passing initial position of a seed), but the second wire makes a 90° turn when entering initial position of the its seed and then grows east [Figs. 15(e) and 16(n)]. In situations $C = (80,4)$ both wires just reflect without forming any conductive bridges or patterns growing from the site of their collision [Figs. 15(f) and 16(o)]. In situations $C = (80,5)$ and $C = (81,5)$ wires pass near each other without interacting [Figs. 15 fm].

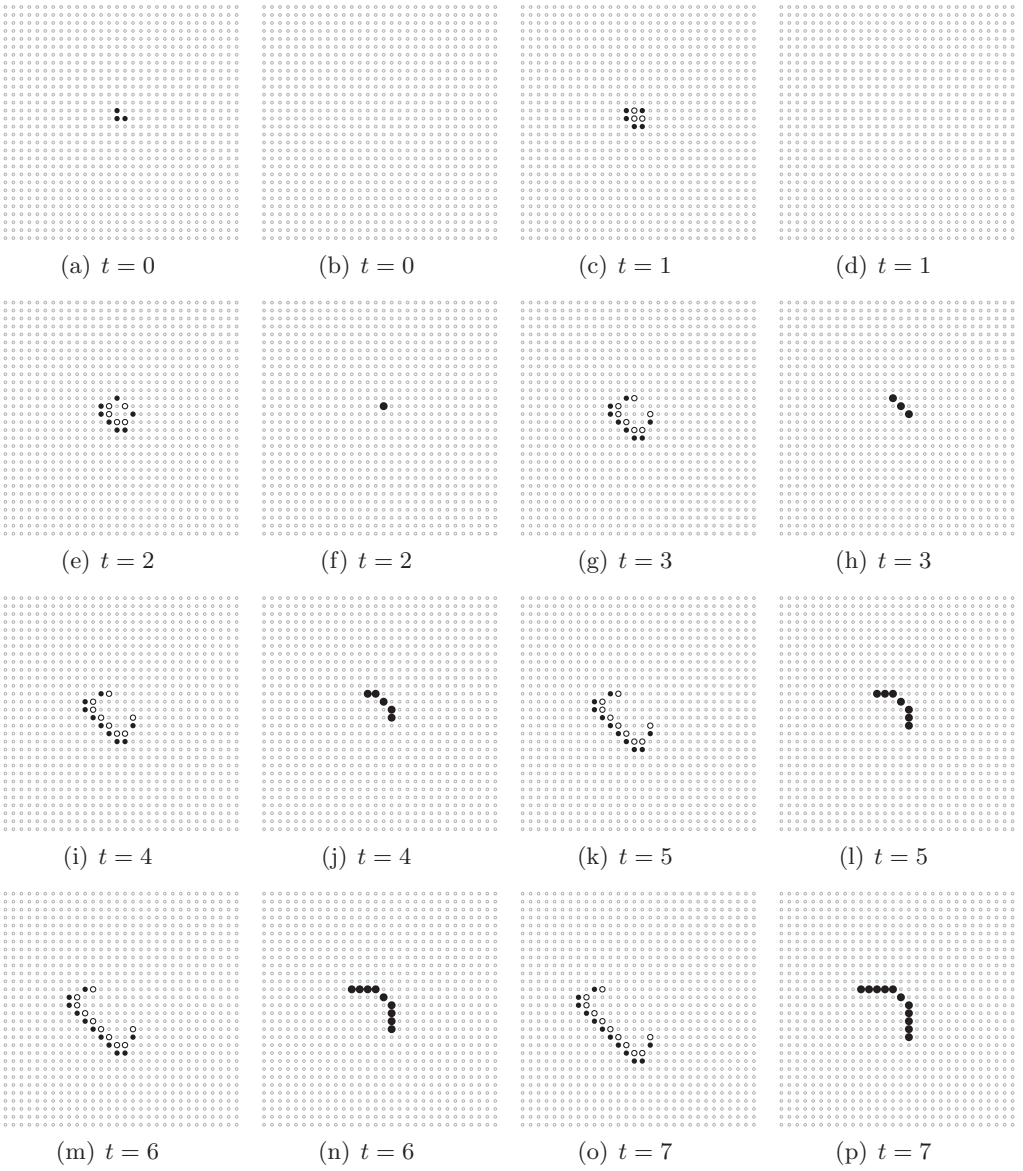

FIG. 12. Production of two wires growing east and south. For each time step t we show excitation (left pattern) and conductivity (right pattern) configurations. In the excitation configurations excited cells are solid black disks, refractory cells are circles. In the conductivity configurations conductive cells are black disks and nonconductive are gray dots.

When the distance between seeds is $C = (81,0)$ the growing wires reflect and detract back to their points of origination. However, when they reach the positions of their seeds a new pattern is formed there [Fig. 15(h)]. It exhibits multithread wires growing northwest, south, and east from the position of the northern seed, and southwest, north, and east from the position of the southern seed [Fig. 16(p)].

An E-shaped configuration of three wires growing east is formed when $C = (81,1)$; the seeds' sites are also connected by a conductive wire [Figs. 15(i) and 16(q)].

Finding 4. By positioning seeds $\begin{smallmatrix} \pm & + \\ & \circ \end{smallmatrix}$ and $\begin{smallmatrix} - & \circ \\ + & + \end{smallmatrix}$ with shift $C = (odd,2)$ it is possible to make a stationary conductive wire between the seeds' locations.

For example, in situation $C = (81,2)$ [Fig. 15(j)] the growing wires collide, make a conductive bridge, and stop their propagation. Thus a stationary wire is formed connecting sites of southern and northern seeds [Fig. 16(r)]. The seeds' sites are connected by a wire in $C = (81,3)$ [Fig. 15(k)] and $C = (81,4)$ [Fig. 15(l)]; however, the wire continues expanding north and south.

To study outcomes of side collisions between wires we position two seeds $\begin{smallmatrix} \pm & + \\ & \circ \end{smallmatrix}$ and $\begin{smallmatrix} - & + \\ \circ & + \end{smallmatrix}$ at distance $C = (h,v)$ [Fig. 17(a)], where h is a number of cells between northernmost excited cells of seeds, and v is a number of cells between northernmost excited cells of seeds. The seed $\begin{smallmatrix} \pm & + \\ & \circ \end{smallmatrix}$ leads to formation of a single-thread wire growing north. The seed $\begin{smallmatrix} - & + \\ \circ & + \end{smallmatrix}$ generates a wire east. Configurations of cells in conductive states developed on 300th step after excitation of automaton with the seeds are shown in Fig. 17.

Colliding wires stop short of touching each other and do not propagate anymore for $C = (60,40)$ and $C = (61,43)$ [Figs. 17(b), 17(k), and 16(a)]. Growth of wire propagating

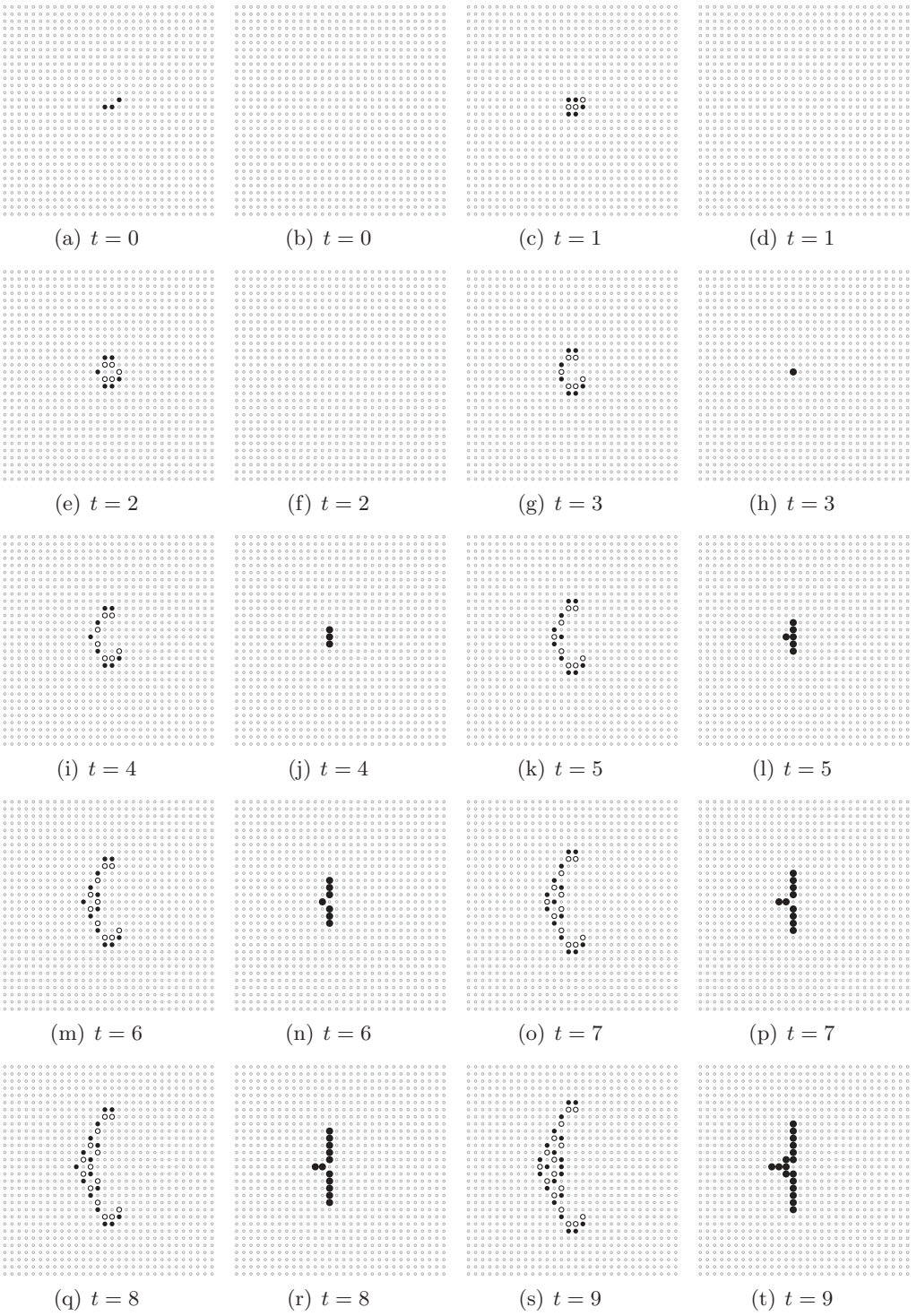

FIG. 13. Three wires growing north, south, and east. For each time step t we show excitation (left pattern) and conductivity (right pattern) configurations. In the excitation configurations excited cells are solid black disks, refractory cells are circles. In the conductivity configurations conductive cells are black disks, and nonconductive are gray dots.

north is canceled by a wire propagating east in $C = (60,42)$ [Fig. 16(b)], and the wires do contact each other [Fig. 17(c)].

In condition $C = (60,43)$ [Fig. 17(d)] two new growing wires are formed as the result of collision of a wire traveling north to a wire traveling east. One new wire propagates west, and another wire propagates east [Fig. 16(c)].

Three new growing wires are formed in the collision of north and east propagating wires when the distance between their seeds is $C = (60,44)$ [Figs. 17(e) and 16(d)] and $C = (61,40)$ [Figs. 17(g) and 16(d)]. One new wire propagates north, and two new wires propagate east. The south wire propagating east is formed when the originally north

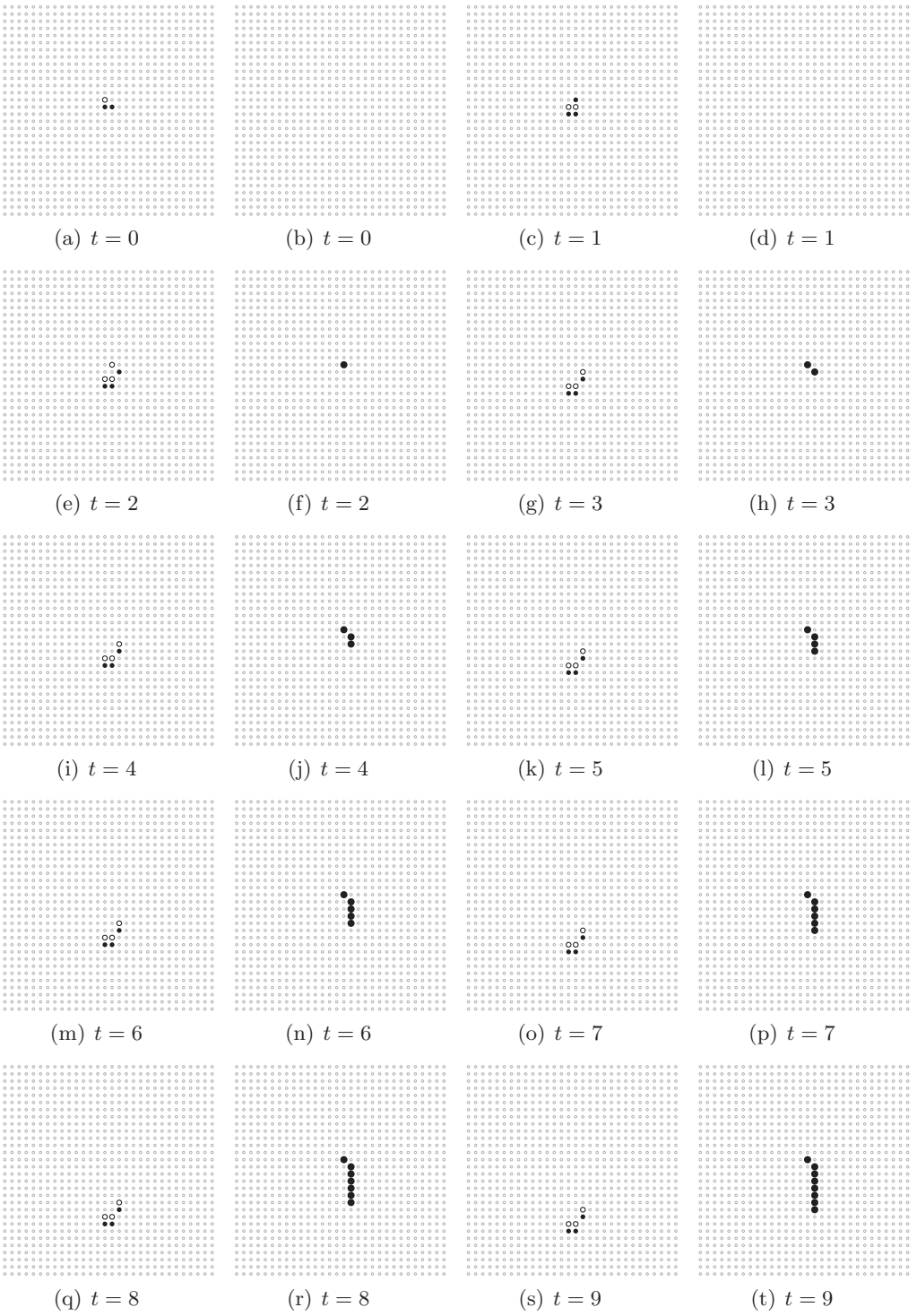

FIG. 14. Single wire grows south. For each time step t we show excitation (left pattern) and coductivity (right pattern) configurations. In the excitation configurations excited cells are solid black disks, refractory cells are circles. In the conductivity configurations conductive cells are black disks, and nonconductive are gray dots.

propagating wire retracts as the result of collision with an originally east propagating wire and is reflected by configurations of excitation interval boundaries imposed by itself.

Almost elastic-like reflection of a wire is observed in case $C = (60,45)$ [Figs. 17(f) and 16(e)]. A wire growing north collides and is canceled by a wire growing east. As the result of impact the east growing wire is reflected and starts growing northeast [Fig. 16(e)].

In situation $C = (61,42)$ both wires retract as the result of collision. However, when they reach the sites of their origination (where cells have already updated boundaries of excitation interval) they are transformed into extended

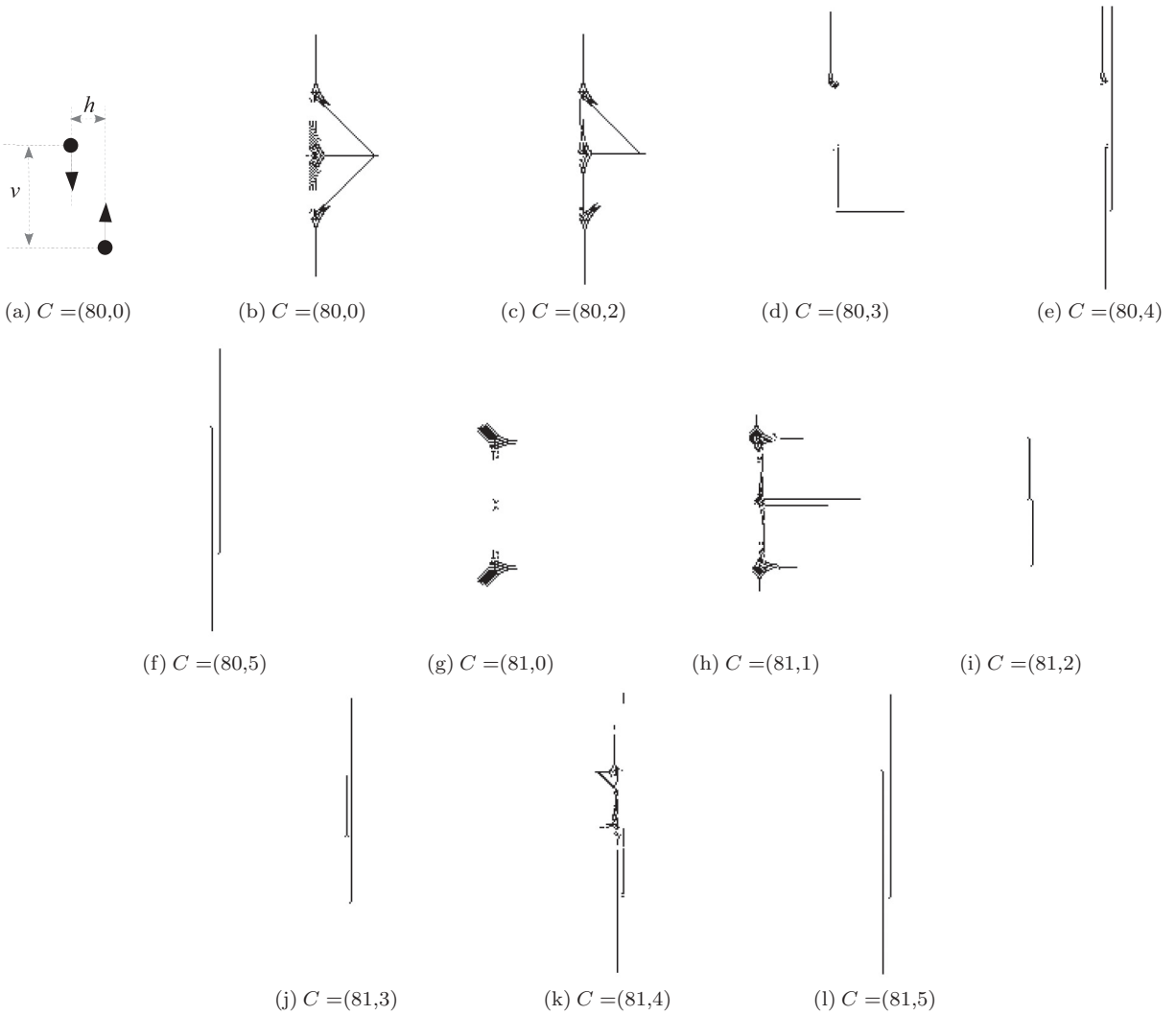

FIG. 15. Head-on collision between wires growing north and south for various distances $C = (h,v)$ between their seeds. h is a number of cells between westernmost excited cells of seeds, and v is a number of cells between northernmost excited cells of seeds. Snapshots of configurations of conductive states are taken at 270th step of iterations. The outcomes of collisions are the same for automata governed by functions $E(1,0,0,0)$ and $E(1,-1,0,0)$.

patterns which give rise to two new wires, both growing south [Figs. 17(g) and 16(j)].

In situation $C = (61,44)$ and $C = (61,45)$ a wire growing north is retracted back to its seed's position as the result of collision with a wire growing east [Figs. 17(h) and 16(h)]. At the same time the wire growing east is reflected and turns north.

Finding 5. It is possible to implement universal routing of conductive wires by positioning seeds of growing wires, and the following operations with wires are implementable:

(1) Formation of stationary wires [Fig. 16(r)]
(2) Stopping of both growing wires [Fig. 16(a)]
(3) Stopping of one wire by another wire without formation of a conductive bridge [Fig. 16(b)]
(4) Formation of conductive circuit with one growing wire [Fig. 16(l)]
(5) Formation of conductive circuit with two growing wires [Figs. 16(c), 16(f), 16(i), 16(k), and 16(m)]
(6) Formation of conductive circuit with three growing wires [Figs. 16(d) and 16(q)]
(7) Reflection of wires without conductive bridging [Figs. 16(h), 16(n), and 16(o)]
(8) Stopping of one wire and reflection of another [Fig. 16(e)]
(9) Co-orientation of both growing wires without formation of a conductive bridge [Fig. 16(g)]
(10) Symmetric reflection and multiplication without formation of conductive bridging [Fig. 16(p)].

V. SUMMARY

We introduced a two-dimensional excitable cellular automaton where resting cells excite depending on whether numbers of their excited neighbors belong to excitation intervals and boundaries of the excitation intervals are updated depending on ratio of excited and refractory cells in each cell's neighborhood. We defined conductivity of a cell via size of its excitation interval and selected the excitation interval update

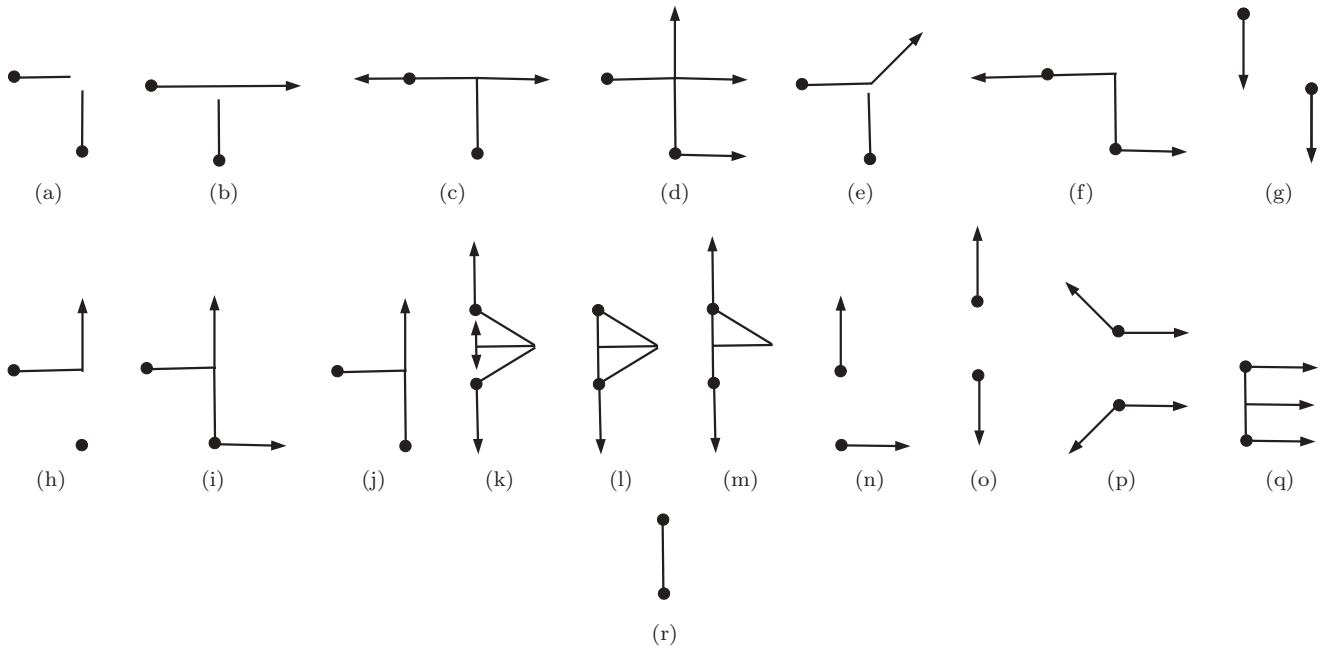

FIG. 16. Schemes of interactions between wires. Initial positions of seeds are shown by black disks. Nongrowing wires are shown by line segments and growing wires by arrows. (a)–(j) Side collision, (k)–(r) head-on collision.

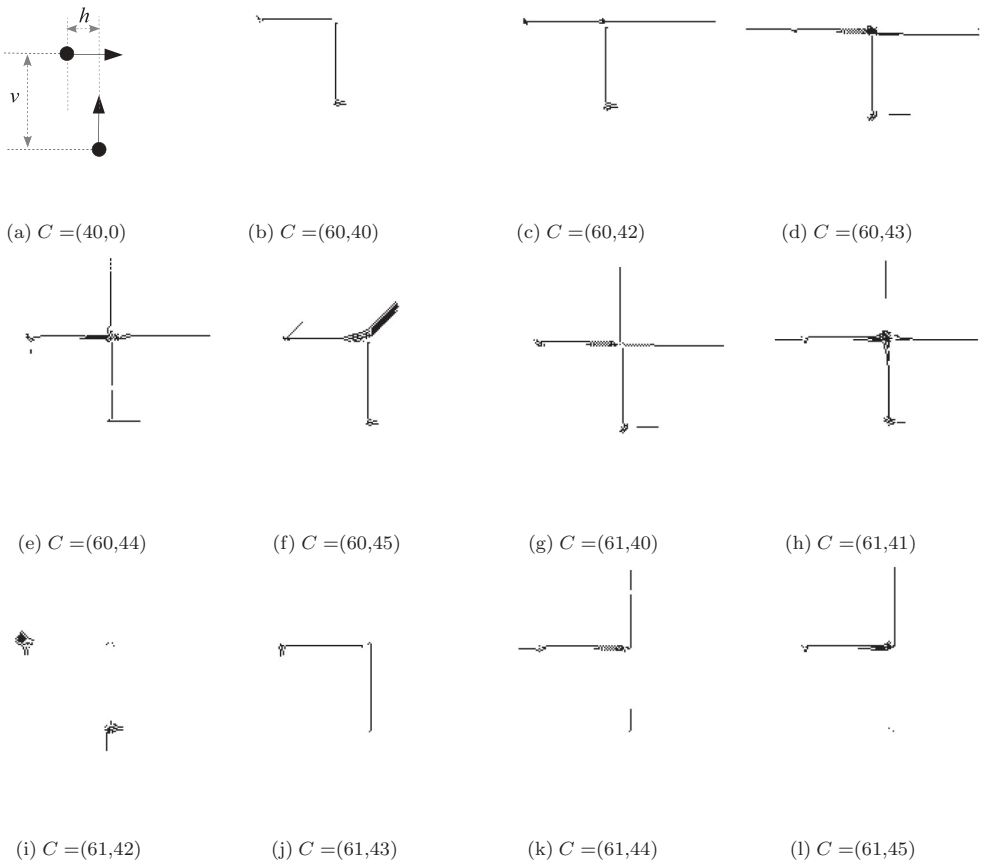

FIG. 17. Side collision between wires growing north and east for various distances $C = (h, v)$ between their seeds. h is a number of cells between northernmost excited cells of seeds, and v is a number of cells between northernmost excited cells of seeds. Snapshots of configurations of conductive states are taken at 300th step of iterations. The outcomes of collisions are the same for automata governed by functions $E(1,0,0,0)$ and $E(1,-1,0,0)$.

functions that lead to formation of connected configurations of conductive cells.

We demonstrated that by positioning elementary seeds of excitation we grow conductive wires (chains of cells in conductive states) and implement routing of the wires via collisions between the wires. Results presented might shed light onto development of information pathways in excitable spatially extended media and contribute towards manufacturing self-growing and self-organizing circuits in ensembles of organic memristive polymers.

Principal findings of the paper are following:

(1) We demonstrated that it is possible to fine tune conductivity of an excitable medium by controlling local dynamics of excitation.

(2) Functions which stabilize excitation dynamics (where size of excitation interval increase with decrease of excitation and decreases when excitation dominates) generate fully conductive when a small number of initially resting cells are stimulated.

(3) A pointwise initial excitation can play the seed of a growing wire or a chain of cells in conductive states; directions of the wire grow in preprogrammed ways in the configuration of the initial excitation

(4) The growing wires can be routed in an almost arbitrary manner, dependent on positions of their seeds

(5) Several wires can interact with each other by changing directions of their growth, merging in a single wire and coaligning.

We show how to design and grow potential information pathways; however. we did not study how the information can be processed in the conductive configurations and circuits. In many cases, extended patterns are formed at the sites of collision between growing wires. Chances are high that these patterns can implement a range of sensible transformations of input excitation to output excitation, which could be interpreted in terms of computation. Computational abilities of the conductive circuits grown in excitable cellular automata will be a major topic of further studies.

[1] A. Ilachinski, *Cellular Automata: A Discrete Universe* (World Scientific, Singapore, 2001).

[2] B. Chopard, and M. Droz, *Cellular Automata Modeling of Physical Systems* (Cambridge University Press, Cambridge, 2005).

[3] M. Gerhardt, H. Schuster, and J. J. Tyson, Physica D **46**, 392 (1990).

[4] M. Markus and B. Hess, Nature (London) **347**, 56 (1990).

[5] A. Adamatzky, B. De Lacy Costello, and T. Asai, *Reaction-Diffusion Computers* (Elsevier, Amsterdam, 2005).

[6] X. Yang, Appl. Math. Model. **30**, 200 (2006).

[7] H. Hartman and P. Tamayo, Physica D **45**, 293 (1990).

[8] J. M. Greenberg and S. P. Hastings, SIAM J Appl. Math. **34**, 515 (1978).

[9] A. Adamatzky and O. Holland, Chaos Solitons Fractals **3**, 1233 (1998).

[10] A. Adamatzky, Int. J. Mod. Phys. C **23**, 1250085 (2012).

[11] L. O. Chua, IEEE Trans. Circuit Theory **18**, 507 (1971).

[12] L. O. Chua and S. M. Kang, Proc. IEEE **64**, 209 (1976).

[13] L. O. Chua, IEEE Trans. Circuits Systems **27**, 1014 (1980).

[14] R. S. Williams, IEEE Spectrum **45**, 29 (2008).

[15] V. Erokhin, arXiv:0807.0333v1 (2008).

[16] J. J. Yang, M. D. Pickett, X. Li, D. A. A. Ohlberg, D. R. Stewart, and R. S. Williams, Nature Nanotechnology **3**, 429 (2008).

[17] V. Erokhin, A. Schüz, and M. P. Fontana, Int. J. Unconventional Comput. **6**, 15 (2010).

[18] D. B. Strukov, G. S. Snider, D. R. Stewart, and R. S. Williams, Nature (London) **453**, 80 (2008).

[19] V. Erokhin, D. Howard, and A. Adamatzky, Int. J. Bifurcation Chaos **22**, 1250283 (2012).

[20] M. Itoh and L. Chua, Int. J. Bifurcation Chaos **19**, 3605 (2009).

[21] A. Adamatzky and L. Chua, Int. J. Bifurcation Chaos **21**, 3083 (2011).

[22] A. Adamatzky and L. Chua, Int. J. Bifurcation Chaos (to be published).

[23] V. Erokhin, T. Berzina, A. Smerieri, A. Camorani, S. Erokhina, and M. P. Fontana, Nano Comm. Netw. **1**, 108 (2010).

[24] M. Bode, A. W. Liehr, C. P. Schenk, and H.-G. Purwins, Physica D **161**, 45 (2002).

[25] G. Grnert, P. Dittrich, K. P. Zauner, ERCIM News **85**, 30 (2011).

[26] A. Adamatzky, J. Holley, P. Dittrich, J. Gorecki, B. De Lacy Costello, K.-P. Zauner, and L. Bull, Biosystems **109**, 72 (2012).

[27] P. H. King, J. C. Corsi, B.-H. Pan, H. Morgan, M. R. de Planque, and K.-P. Zauner, Biosystems **109**, 18 (2012).

[28] J. Szymanski, J. N. Gorecka, Y. Igarashi, K. Gizynski, J. Gorecki, K.-P. Zauner, and M. D. Planque, Int. J. Unconventional Comput. **7**, 185 (2011).